End-milling of Inconel 718 Superalloy - An Analytical Modelling

A Moufki, Gael Le Coz, D Dudzinski

Available online at www.sciencedirect.com

ScienceDirect

Procedia CIRP 58 (2017) 358 – 363

www.elsevier.com/locate/procedia

16th CIRP Conference on Modelling of Machining Operations

End-milling of Inconel 718 superalloy - An analytical modelling

A. Moufki[a]*, G. Le Coz[a] , D. Dudzinski[a]

[a]*Laboratoire d'Etude des Microstructures et de Mécanique des matériaux, LEM3, UMR-CNRS 7239, Université de Lorraine, 4 rue Fresnel, Metz, 57070, France*

* Corresponding author. Tel: (33)3 87 37 42 90, fax: (33)3 87 31 53 66. E-mail address: abdelhadi.moufki@univ-lorraine.fr

Abstract

In this work, a predictive machining theory, taking into account the thermo-visco-plastic response of the work material, is applied to the end milling process. In order to consider the particular conditions of end-milling operation, when the uncut chip thickness becomes in range of the cutting edge radius, the cutting edge effect has been also introduced. The proposed model appears as an interesting alternative to the mechanistic approach which requires many experimental tests to determine the milling cutting force coefficients. The predicted cutting forces are in good agreement with experimental data for dry machining of Inconel 718.

Peer-review under responsibility of the scientific committee of The 16th CIRP Conference on Modelling of Machining Operations

Keywords: analytical model, end-milling, cutting edge effect

1. Introduction

End-milling process is widely used in aerospace industry and in dies and molds manufacturing. However, under certain cutting conditions, the machined surface can be deteriorated by different phenomena as excessive cutter deflection, machine tool chatter and tool wear. Due to its high temperature strength and high corrosion resistance, Inconel 718 superalloy is widely employed in the aerospace industry, in particular in the hot sections of gas turbine engines. It is known as being among the most difficult-to-cut materials. The goal for the machining manufacturers is to improve material removal rate with high speed machining and to move toward dry cutting by eliminating or minimizing the use of cutting fluids. Due to the extreme thermomechanical loads during machining of Inconel 718 superalloy, much attention should be paid to surface integrity: metallurgical alterations including microstructural distortion, phase transformations, heat affected layers and tensile residual stresses, [1-4]. Residual stress is one of the most relevant practical parameters to evaluate the machined surface quality, especially when critical structural components are machined, [5-6], the residual stress distributions were studied in quasi orthogonal cutting operation of Inconel 718. At high cutting speeds, a thin layer with tensile residual stresses has been observed near the machined surface, exhibiting a maximum tensile stress at the surface. Similar stress profiles were found during high speed dry milling by [7-9] studied residual stresses in milling of Inconel 718 for two grades of coated carbide cutting tools. The authors have observed small values of residual stresses, which are mostly compressive for coated carbide cutting inserts with round shape, chamfered cutting edge, negative rake angle and small radius generate.

Because of the complex milling process geometry, empirical approaches are often used to select machining parameters and they can lead to suboptimal solutions. Therefore, a predictive model of cutting forces may be very useful for the cutting process optimisation. In the literature, the major works are based on the mechanistic approach. In this approach, the cutting forces are calculated by using cutting force coefficients (or specific pressures) which are calibrated from experimental data [10-13]. Since these coefficients depend on cutting conditions, cutting tool geometry and tool-workpiece materials, the mechanistic models require a lot of experimental tests. Altintas and Spence [14] presented closed form expressions to calculate the helical end milling forces

Peer-review under responsibility of the scientific committee of The 16th CIRP Conference on Modelling of Machining Operations
doi:10.1016/j.procir.2017.03.330

more accurately and Yucesan and Altintas [15] developed a mechanistic model by including the influence of instantaneous chip thickness and rake angle into the milling force coefficients.

An alternative way to determine the milling cutting force coefficients is to use an orthogonal cutting data base and an analytical model of oblique cutting associated to the milling process, see [16-19]. Another possibility is to apply the Oxley's predictive orthogonal cutting theory extended to oblique cutting, [20], such as in Li and Li [21]. However, it should be noted that in this approach, a sticking contact independent of the workpiece-tool materials was assumed at the tool-chip interface. In addition, the predictive machining theory is based on several empirical relations whose coefficients have to be determined. In [22] a cutting forces model for milling Inconel 718 alloys was presented.

The aim of the present work is to propose an alternative approach through a thermo-mechanical model of oblique cutting applied to the end-milling process. Moreover, this analytical approach was extended to the case where the material flow through the primary shear zone is analyzed with respect to a non-inertial reference frame, [23]. For each infinitesimal cutting edge element, the elementary chip is obtained from an oblique cutting process where the chip formation is supposed to occur mainly by shearing within a thin zone, the primary shear band. The thermomechanical behavior of the workpiece material and the friction at the tool-chip interface are considered. The cutting edge effect is also added to take into account of the particular conditions of end-milling process. To validate the modelling approach, experimental end-milling tests were performed on Inconel 718 in dry conditions.

Nomenclature

ω	angular velocity
α_h	helix angle
α_r	radial angle
α_n	normal rake angle
R	tool radius
N_t	number of teeth
V	cutting speed
φ_i	angular position for the i^{th} tooth
φ_{en}	entrance angle
φ_{out}	exit angle
d_r	radial depth of cut
d_a	axial depth of cut
t_1	undeformed chip thickness
λ_s	edge inclination angle
dF_t, dF_r, dF_a	elementary cutting, thrust and lateral forces exerted on the cutting edge
K_{tc}, K_{rc}, K_{ac}	cutting force coefficients
K_{te}, K_{re}, K_{ae}	edge force coefficients

2. Cutting force model for end milling operation

In this paper, a thermomechanical model is used to predict the cutting forces in peripheral end milling. The machining operation is analyzed with respect to the frame (**x**, **y**, **z**) as shown in figure 1. For a position z , an infinitesimal cutting edge element produces an elementary chip from an oblique cutting operation which is modelled by using the thermomechanical approach developed in [24,25]. Although this predictive machining theory was established for stationary conditions, it could be applied to milling processes by using the assumption that at each instant of time the chip formation can be modelled by an equivalent stationary process [26].

For a point of cutting edge, at position z , of the i^{th} cutting tooth, the angular position $\varphi_i(z)$ from the **x** -axis is reported in figure 1 and determined by:

$$\varphi_i(z) = \omega t - \frac{z}{R}\tan\alpha_h + (i-1)\frac{2\pi}{N_t} \tag{1}$$

where N_t, $\omega(rad/s)$, α_h and R represent respectively the number of teeth, the cutter angular velocity, the helix angle and the tool radius. According to the kinematics of milling process, the i^{th} flute goes into cut when:

$$\varphi_{en} < \varphi_i(z=0) < \left(\varphi_{ex} + \frac{d_a}{R}\tan\alpha_h\right) \tag{2}$$

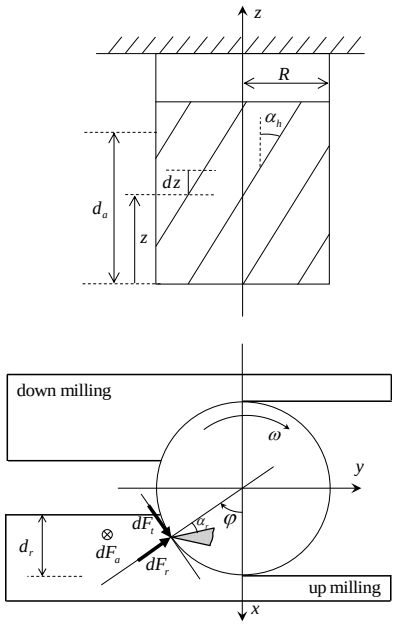

Fig. 1. Peripheral milling process.

with φ_{en} and φ_{ex} represent respectively the angle at which the cutter enters the cut and the angle at which the cutter exits the cut:

$$\begin{cases} \varphi_{en} = 0 \quad \text{and} \quad \varphi_{ex} = \pi \\ \text{for slot milling} \quad (\text{full immersion}) \\ \varphi_{en} = 0 \quad \text{and} \quad \varphi_{ex} = \cos^{-1}(1 - d_r / R) \\ \text{for up-milling} \\ \varphi_{en} = \pi/2 + \sin^{-1}(1 - d_r / R) \quad \text{and} \quad \varphi_{ex} = \pi \\ \text{for down-milling} \end{cases} \tag{3}$$

The axial depth of cut d_a and the radial depth of cut d_r are reported in Fig. 1.

During milling process, the interaction between the tool and chip is generally due to two main mechanisms, cutting with rake face and cutting edge effect. The last one becomes dominant when the uncut chip thickness is in range of the cutting edge radius such as in milling processes. To model end milling process, the helical flutes are divided into small differential oblique cutting edge segments. The cutting forces, due to the tool rake, exerted on each cutting edge element are often supposed to be proportional to the undeformed chip section which is determined from Martelloti's equation [27]. At every instant of time, the total force components acting on a flute are obtained by integrating the elementary force components exerted on the individual discs.
In milling operations, the tangential (dF_t), radial (dF_r) and axial (dF_a) forces acting on a differential flute element with height *dz*, see Fig. 1, are generally modeled as follows:

$$\begin{cases} dF_t = (K_{te} + K_{tc}\ f_t \sin\varphi_i)\, dz \\ dF_r = (K_{re} + K_{rc}\ f_t \sin\varphi_i)\, dz \\ dF_a = (K_{ae} + K_{ac}\ f_t \sin\varphi_i)\, dz \end{cases} \tag{4}$$

The coefficients K_{tc}, K_{rc} and K_{ac} correspond to the cutting mechanism with the tool rake face. In the present work, these coefficients are determined from a predictive machining model of oblique cutting [23] :

$$\begin{cases} K_{tc} = \dfrac{\tau_h \cos\eta_s \left(\cos\alpha_n \cos\lambda_s + \tan\lambda \left(\sin\eta_c \sin\lambda_s + \cos\eta_c \sin\alpha_n \cos\lambda_s\right)\right)}{\cos\lambda_s \sin\phi_n \left(\cos(\phi_n - \alpha_n) - \tan\lambda \cos\eta_c \sin(\phi_n - \alpha_n)\right)} \\ K_{rc} = \dfrac{\tau_h \cos\eta_s \left(-\sin\alpha_n + \tan\lambda \cos\eta_c \cos\alpha_n\right)}{\cos\lambda_s \sin\phi_n \left(\cos(\phi_n - \alpha_n) - \tan\lambda \cos\eta_c \sin(\phi_n - \alpha_n)\right)} \\ K_{ac} = \dfrac{\tau_h \cos\eta_s \left(\cos\alpha_n \sin\lambda_s + \tan\lambda \left(-\sin\eta_c \cos\lambda_s + \cos\eta_c \sin\alpha_n \sin\lambda_s\right)\right)}{\cos\lambda_s \sin\phi_n \left(\cos(\phi_n - \alpha_n) - \tan\lambda \cos\eta_c \sin(\phi_n - \alpha_n)\right)} \end{cases} \tag{5}$$

where τ_h, η_{sh} and η_c represent respectively the shear stress at the exit of the primary shear zone (PSZ), the shear direction in the PSZ and the chip flow angle and they are obtained from the thermomechanical approach as in[28-30]. Note that the oblique cutting conditions corresponding to a cutting edge element of the i^{th} cutting tooth are given by:

$$\begin{aligned} &\lambda_s = \alpha_h, \quad f_t \sin(\varphi_i) : \textit{uncut chip thickness} \\ &\alpha_n = \tan^{-1}(\tan(\alpha_r)\cos\alpha_h), \quad V = \omega R \end{aligned} \tag{6}$$

with λ_s, f_t, V, α_n and α_r correspond respectively to the inclination angle, the feed per tooth, the cutting speed, the normal rake angle and the radial rake angle.

In addition, the edge cutting coefficients K_{te}, K_{re} and K_{ae} represent the rubbing forces between the tool and the workpiece [31]. The coefficients K_{te} and K_{re} are usually determined from orthogonal cutting data for a tool-workpiece couple and for appropriate cutting conditions. It can also be noted that K_{ae} is known to be very small in oblique cutting and it is often taken as zero [32].

In the x, y and z directions, the components of the elementary cutting forces are given by :

$$\begin{cases} dF_x = dF_t(\varphi)\sin\varphi - dF_r(\varphi)\cos\varphi \\ dF_y = dF_t(\varphi)\cos\varphi + dF_r(\varphi)\sin\varphi \\ dF_z = -dF_a(\varphi) \end{cases} \tag{7}$$

Thus, the total forces exerted on the tool are obtained by integrating the elementary force components (7) along the axial direction z :

$$\begin{cases} F_x = \sum_{i=1}^{N_t} \int_{z_{\min}}^{z_{\max}} \left\{ f_t \left(K_{tc} \sin^2(\varphi_i) - K_{rc} \sin(\varphi_i)\cos(\varphi_i)\right) + \left(K_{te} \sin(\varphi_i) - K_{re} \cos(\varphi_i)\right)\right\} dz \\ F_y = \sum_{i=1}^{N_t} \int_{z_{\min}}^{z_{\max}} \left\{ f_t \left(-K_{tc} \sin(\varphi_i)\cos(\varphi_i) - K_{rc} \sin^2(\varphi_i)\right) - \left(K_{te} \cos(\varphi_i) + K_{re} \sin(\varphi_i)\right)\right\} dz \\ F_z = \sum_{i=1}^{N_t} \int_{z_{\min}}^{z_{\max}} f_t K_{ac} \sin(\varphi_i)\, dz \end{cases} \tag{8}$$

where $z_{\min}$ and $z_{\max}$ represent respectively the axial boundaries of the engaged part of the i^{th} flute during cutting. Considering the differential equation

$$dz = -R\, d\varphi / \tan\alpha_h \tag{9}$$

deduced from (1), equation (8) can be integrated as follows

$$\begin{cases} F_x = \sum_{i=1}^{N_t} \dfrac{R}{\tan\alpha_h} \left(f_t \left\{A_c K_{tc} - B_c K_{rc}\right\} + \left\{A_e K_{te} - B_e K_{re}\right\}\right) \\ F_y = \sum_{i=1}^{N_t} \dfrac{R}{\tan\alpha_h} \left(-f_t \left\{B_c K_{tc} + A_c K_{rc}\right\} - \left\{B_e K_{te} + A_e K_{re}\right\}\right) \\ F_z = \sum_{i=1}^{N_t} \dfrac{R}{\tan\alpha_h} f_t K_{ac} A_e \end{cases} \tag{10}$$

with :

$$\begin{cases} A_c = \frac{1}{2}\left(\varphi_i^{z_{min}} - \varphi_i^{z_{max}}\right) + \frac{1}{4}\left(\sin(2\varphi_i^{z_{max}}) - \sin(2\varphi_i^{z_{min}})\right) \\ A_e = \cos(\varphi_i^{z_{min}}) - \cos(\varphi_i^{z_{max}}) \\ B_c = \frac{1}{2}\left(\cos(2\varphi_i^{z_{min}}) - \cos(2\varphi_i^{z_{max}})\right) \\ B_e = \sin(\varphi_i^{z_{min}}) - \sin(\varphi_i^{z_{max}}) \end{cases} \quad (11)$$

where the angles $\varphi_i^{z_{min}}$ and $\varphi_i^{z_{max}}$ are determined from (1-3) and represent respectively the angular positions of the axial boundaries z_{min} and z_{max} :

$$\begin{cases} \varphi_i^{z_{min}} = \min\left(\omega t + (i-1)\frac{2\pi}{N_t},\ \varphi_{ex}\right) \\ \varphi_i^{z_{max}} = \max\left(\varphi_{en},\ \omega t - \frac{d_a}{R}\tan\alpha_h + (i-1)\frac{2\pi}{N_t}\right) \end{cases} \quad (12)$$

3. Model validation

The present model was applied to the peripheral milling of Inconel 718. Experiments were carried out on a high speed machining center Roeders RP600. A four teeth Hitachi EPP-4120-05-TH end mill of 12 mm diameter was used. The helix angle was 43° and the rake angle was 0°. The tool was a PVD TiSiN nano-coating deposited on micro-grain carbide.

Table 1. Cutting tool characteristics.

Tool	EPP-4120-05-TH	Helix angle (°)	43
Diameter (mm)	12	Radial angle (°)	0
Tooth	4	Coating	PVD TiSiN

The workpiece material was a solution treated and aged Inconel 718 alloy, with hardness of 38HRC. The standard chemical composition is 50–55%Ni, 0.02–0.08%C, 17–21%Cr, 0.7–1.15%Ti, 4.8–5.5% Nb+Ta,0.3–0.7%Al, 2.8–3.3%Mo, 0.35max%Si, 1% max Co [33]. The work material was supplied in parallelepiped form of 50 mm length, 8 mm height and 75 mm width. The width was reduced of radial depth of cut after each cutting test. A specific set up was developed to perform only peripheral milling operations, on the 8 mm height of the specimens and without action of the flat cutting edge. It was mounted on a dynamometric table Kistler 9265B, associated with a charge amplifier Kistler 5017B and a NI data acquisition system, to measure the cutting forces during the process.

Cutting conditions were chosen from previous study [35] with moderate cutting speed values of 40, 60 and 80 m/min. Down milling operations were performed with a feed rate of 0.07 mm/tooth, an axial depth of cut of 8 mm, and a radial depth of cut equal to 1 mm.

Table 2. Cutting condition.

Cutting speed V (m/min)	40, 60, 80
Feed f_t (mm/th)	0.07
Axial depth d_a (mm)	8
Radial depth d_r (mm)	1
Lubricant	dry

Since the axial depth of cut d_a is large enough (i.e. $d_a \geq \tan\alpha_h / R > (\varphi_{ex} - \varphi_{en})$), the evolution of the cutting forces F_x, F_y and F_z present a quasi stationary regime where the cutting operation remains constant (the engaged cutting edges change but the total uncut chip thickness does not change), see figure 2.

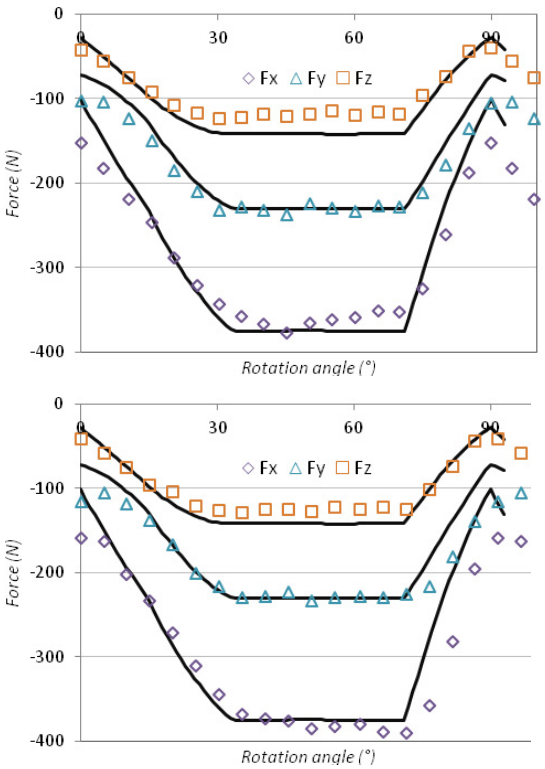

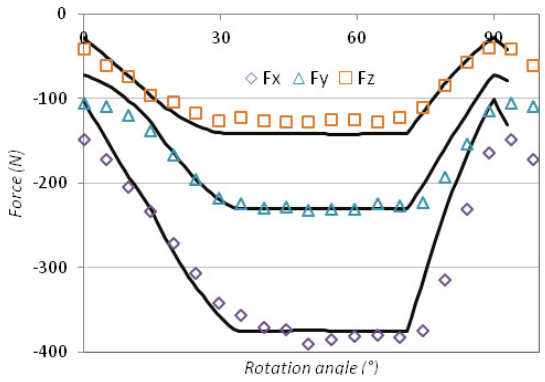

Fig. 2. Comparison between predicted (lines) and experimental forces (symbols) for cutting speeds of (a) 40 m/min (b) 60 m/min and (c) 80 m/min.

In addition, according to the dry orthogonal tests performed in [17], for uncoated tool and AlTiN coated tool, it appears that the mean friction angle becomes almost constant ($\lambda \simeq 26,5°$) for $50 \le V \le 200\ m/min$ and $feed\ rate = 0.1, 0.2\ mm/rev$. In the following, λ was taken constant.

In the present work, the coefficients K_{te} and K_{re} are determined from the experimental cutting forces by considering that the coefficients K_{tc}, K_{rc} and K_{ac} are obtain for the predictive machining theory [23] where the thermomechanical response of the work-material is supposed to be described by the Johnson-Cook law [34]. Thus, we get:

$$\begin{cases} \left|F_x^{\exp} - F_x^{\mathrm{mod}}\right| = \dfrac{R}{\tan\alpha_h}\left(K_{te}\sum_{i=1}^{N_t} A_e - K_{re}\sum_{i=1}^{N_t} B_e\right) \\ \left|F_y^{\exp} - F_y^{\mathrm{mod}}\right| = \dfrac{-R}{\tan\alpha_h}\left(K_{te}\sum_{i=1}^{N_t} B_e + K_{re}\sum_{i=1}^{N_t} A_e\right) \end{cases} \quad (12)$$

With $F^{\exp}$ and F^{mod} represent respectively the experimental and model forces.

According to this calibration procedure, we obtain: $K_{te} = 19\ N/mm$ and $K_{te} = 39\ N/mm$. From Fig. 2, it appears that the model predictions are in good agreement with the experimental results. In addition, it can be observed that the cutting velocity has a weak effect on the cutting forces. This tendency confirms the fact that the friction coefficient can be supposed to be constant.

4. Conclusion

In this work, we present an approach based on the coupling between a *thermomechanical predictive machining theory* and a *new method for the determination of cutting edge effect from one cutting test*. For each infinitesimal cutting edge element, the elementary chip is obtained from an oblique cutting process. The thermomechanical behaviour of the workpiece material and the friction at the tool-chip interface are considered. To obtain the effect of cutting edge on the cutting forces, we propose a systematic method allowing to determine the appropriate cutting conditions for which the evolution of cutting forces is quasi-stationary (i.e. the engaged cutting edges change but the total uncut chip thickness does not change. Thus, the cutting forces remain constant, see figure 2). The proposed model permits also to analyze the local parameters such as the cutting temperatures, the tool-chip contact length and the chip flow direction. Therefore, it represents a real alternative to the mechanistic approach, used in the majority of works on milling processes, and requires many experimental tests to determine the milling cutting force coefficients. To validate the modelling approach, experimental end-milling tests were performed on Inconel 718 in dry conditions. The predicted cutting forces are in good agreement with experimental data over a wide range of cutting conditions.

References

[1] Field M, Khales JF. Review of surface integrity of machined components. Annals of CIRP 1971; 20 (2): 153–163.
[2] Arunachalam RM, Mannan MA, Spowage AC. Surface integrity when machining age hardened Inconel 718 with coated cutting tools. International Journal of Machine tools and Manufacture 2004; 44: 1481–1491.
[3] Brinkmeier E, Cammet JT, König W, Leskovar P, Peters J, Tönshoff K. Residual stresses, measurement and causes in machining processes. Annals of the CIRP 1982; 31 (2): 491–510.
[4] Guo YB, Li W, Jawahir IS. Surface integrity characterization and prediction in machining of hardened and difficult-to-machine alloys: a state-of-art research review and analysis. Machining Science and Technology 2009; 13: 437–470.
[5] Outeiro JC, Pina JC, M'Saoubi R, Pusavec F, Jawahir IS. Analysis of residual stresses induced by dry turning of difficult-to-machine materials. CIRP Annals – Manufacturing Technology 2008; 57: 77–80.
[6] Schlauer C, Peng RL, Odén M. Residual stresses in a nickel-based superalloy introduced by turning. Materials Science Forum 2002; 404–407: 173–178.
[7] Derrien S, Vigneau J. High speed milling of difficult to machine alloys. A. Molinari, H. Schulz, H. Schulz (Eds.), Proceedings of the 1st French and German Conference on High Speed Machining, University of Metz-France 1997.
[8] Guerville L, Vigneau J. Influence of machining conditions on residual stresses. D. Dudzinski, A. Molinari, H. Schulz (Eds.), Metal Cutting and High Speed Machining, Kluwer Academic/Plenum Publishers 2002:, 201–210.
[9] Ng EG, Soo SL, Sage C, Dewes RC, Dewes R, Aspinwall DK. High speed ball nose end milling of Inconel 718 with variable tool geometry, experimental and finite element analysis. D. Dudzinski, A. Molinari, H. Schulz (Eds.), Metal Cutting and High Speed Machining, Kluwer Academic/Plenum Publishers 2002: 191–200.
[10] Tlusty J, MacNeil P. Dynamics of cutting forces in end milling. CIRP Annals 1975; 24 (1): 21-25.
[11] Kline WA, DeVor RE, Zdeblick WJ. A mechanistic model fort he force system in end milling with application to machining airframes structures. Proc. of the 8th North American Manufacturing Res Conf. 1980; 8: 297.
[12] Kline WA, DeVor RE. The effect of runout on cutting geometry and forces in end milling. International Journal of Machine tool and Research 1983; 23 (2-3): 123-140.
[13] Sutherland J, DeVor RE. An improved method for cutting force and surface error prediction in flexible end milling systems. Journal of Engineering for Industry, Transactions of the ASME 1986; 108: 269-279.
[14] Altintas Y, Spence A. End milling force algorithms for CAD systems. CIRP Annals 1991; 40(1): 31-34.
[15] Yucesan G, Altintas Y. Improved modelling of cutting coefficients in peripheral milling. International Journal of Machines Tools Manufacturing 1994; 34 (4): 473-487.
[16] Budak E, Altintas Y, Armarego EJA. Prediction of milling force coefficients from orthogonal data. Journal of Manufacturing Science and Engineering 1996; 118: 216-224.
[17] Armarego EJA, Brown RH. The machining of metals. Prentice Hall , New York, 1969.

[18] Armarego EJA, Whitfield RC. Computer based modelling of popular machining operations for forces and power prediction. Annals of the. CIRP 1985; 34(1): 65-69.
[19] Armarego EJA, Deshpande NP. Computeriezd Cutting models for forces in end milling including eccentricity effects. Annals of the CIRP 1989; 38 (1): 45-49.
[20] Oxley PLB. An analytical approach to assessing machinability. Ellis Horwood, 1989.
[21] Li HZ, Zhang WB , Li XP. Modelling of cutting forces in helical end milling using a predictive machining theory. International Journal of Mechanical Sciences 2001; 43 (8):1711-1730.
[22] Li HZ, Wang J. A cutting forces model for milling Inconel 718 alloy based on a material constitutive law. Proc. IMechE, Part C: Journal of Mechanical Engineering Science 2013; 227(8): 1761-1775.
[23] Moufki A, Dudzinski D, Le Coz G. Prediction of cutting forces from an analytical model of oblique cutting, application to peripheral milling of Ti-6Al-4V alloy. International Journal of Advanced Manufacturing Technology 2015; 81 (1-4): 615-626.
[24] Moufki A, Dudzinski D, Molinari A, Rausch M. Thermoviscoplastic modelling of oblique cutting: forces and chip flow predictions. International Journal of Mechanical Sciences 2000; 42 (6): 1205-1232.
[25] Moufki A, Devillez A, Dudzinski D, Molinari A. Thermomechanical modelling of oblique cutting and experimental validation. International Journal of Machine Tools and Manufacture 2004; 44 (9): 971-989.
[26] Li HZ, Li XP. Milling force prediction using a dynamic shear length model. International Journal of Machine Tools and Manufacture 2002; 42 (2): 277-286.
[27] Martelotti ME. An analysis of milling process. Transactions of ASME 1941; 63: 677-700.
[28] Molinari A, Moufki A. A new thermomechanical model of cutting applied to turning operations. Part I. Theory. Int. J. Mach. Tools Manuf. 2005; 45(2): 166–180.
[29] Moufki A, Molinari A. A new thermomechanical model of cutting applied to turning operations. Part II. Parametric study. Int. J. Mach. Tools Manuf. 2005; 45(2): 181–193.
[30] Moufki A, Devillez A, Segreti M, Dudzinski D. A semi-analytical model of non-linear vibrations in orthogonal cutting and experimental validation. International Journal of Machine Tools and Manufacture 2006; 46 (3–4): 436-449.
[31] Altintas Y. Manufacturing Automation: Metal Cutting Mechanics, Machine Tool Vibrations, and CNC Design. Cambridge University Press, 2000.
[32] Armarego EJA, Whitfield RC. Computer based modelling of popular machining operations for forces and power prediction. CIRP Annals 1985; 34(1): 65-69.
[33] Devillez A, Le Coz G, Dominiak S, Dudzinski D. Dry Machining of Inconel 718, workpiece surface integrity. Journal of Material Processing Technology 2011; 211 (10): 1590-1598.
[34] Uhlmann E, von der Schulenburg MG, Zettier R. Finite element modeling and cutting simulation of inconel 718. CIRP Annals – Manufacturing Technology 2007; 56: 61–64.
[35] Le Coz G, Dudzinski D. Temperature variation in the workpiece and in the cutting tool when dry milling Inconel 718. International Journal of Advanced Manufacturing Technology 2014; 74(5-8): 1133-1139.